carbonate does not lead to the stabilization of the +2 oxidation state.[11b] It can be considered that the larger size of the +2 ions leads to smaller steric interactions between the two cycles of sandwich complexes and thus to an increased stability. Also, as mentioned above in the discussion of the stability of sandwich complexes with **1**, van Remoortere et al.[20] found that the 1:2 sodium adduct with this ligand adopts a particularly stable conformation in the solid state and the authors of the present work reported[9] that this complex is significantly more stable than the complexes formed by the other alkali-metal ions. For a coordination number of eight, the ionic radius of ytterbium increases from 0.98 to 1.14 Å when the metal is reduced from the trivalent to the divalent oxidation state;[18] the new ionic radius is then very near that of Na^+ (1.18 Å). The high stability of the Yb(II) sandwhich complex with **1** might thus be ascribed partially to the formation of an adduct with a conformational arrangement similar to the one of the sodium 1:2 complex.

One of the largest shifts toward the positive potentials (around 300 mV) has been obtained in the reduction of the samarium complex with the very large macrocycle **5**. The cation Yb(II) is also stabilized by this ligand but to a smaller degree. It can be assumed that the divalent ions are better able to fill the internal cavity of **5** when this ligand is in a "wrap around" conformation; these ions are thus complexed more strongly. Furthermore, intraligand repulsions are probably smaller for the Sm(II) complex than for the Yb(II) complex, and accordingly, the stability of the former is higher.

Concluding Remarks

The chemistry of the lanthanides has been thoroughly investigated[8] and the complexation of these metals by a variety of ligands has been shown to follow some common trends, namely that the stability of the complexes increases more or less regularly when the ionic radius decreases and that the divalent lanthanides are involved in less-stable complexes than the trivalent ions. Because of their peculiar structure, the macrocyclic lanthanide complexes exhibit an entirely different behavior which is often quite unexpected. The novel chemistry of the crown ethers, as described in the present paper, is a new addition to the already long list of exciting properties of the macrocycles.[1,2]

Acknowledgment. We gratefully acknowledge financial support from the Fonds National de la Recherche Scientifique of Belgium. J.F.D. is Chercheur Qualifié at this institution.

Registry No. 1, 294-93-9; **2**, 33100-27-5; **3**, 15196-73-3; **5**, 17455-25-3; Pb, 7439-92-1; Tl, 7440-28-0; La, 7439-91-0; Ce, 7440-45-1; Pr, 7440-10-0; Nd, 7440-00-8; Sm, 7440-19-9; Gd, 7440-54-2; Tb, 7440-27-9; Dy, 7429-91-6; Ho, 7440-60-0; Er, 7440-52-0; Tm, 7440-30-4; Yb, 7440-64-4; Lu, 7439-94-3.

Liquid-Crystalline Solvents as Mechanistic Probes. 8. Dynamic Quenching of Pyrene Fluorescence by Pyrene in the Liquid-Crystalline and Isotropic Phases of a Cholesteric Solvent[1]

Valerie C. Anderson, Bruce B. Craig, and Richard G. Weiss*

Contribution from the Department of Chemistry, Georgetown University, Washington, D.C. 20057. *Received July 20, 1981*

Abstract: Rate constants and activation parameters for the quenching of pyrene fluorescence by pyrene have been determined in the cholesteric and isotropic phases of a 59.5/15.6/24.9 (w/w/w) mixture of cholesteryl oleate/cholesteryl nonanoate/cholesteryl chloride. From the small differences in the energies and entropies of activation (E_3(cholesteric) = 9.3 ± 0.3 kcal/mol and E_3(isotropic) = 7.0 ± 0.4 kcal/mol; $\Delta S^{\ddagger}$(cholesteric) = 5 ± 2 eu and $\Delta S^{\ddagger}$(isotropic) = −2 ± 3 eu), it is concluded that cholesteric solvent order has little effect on the quenching efficiency. The influence of solvent anisotropy on the efficiency of this process is compared to that observed with other reactions which are retarded or enhanced by solvent order.

Recently, we concluded from dynamic quenching data obtained in the cholesteric and isotropic phases of a 59.5/15.6/24.9 (w/w/w) mixture of cholesteryl oleate/cholesteryl nonanoate/cholesteryl chloride (CM) that the preferred orientation for the quenching of pyrene fluorescence by 5α-cholestan-3β-yldimethylamine (CA) is very specific and resembles closely the commonly accepted exciplex configuration.[2] In this study, we have employed similar techniques to probe the sensitivity of pyrene fluorescence quenching by pyrene (P) to liquid-crystalline order.

Previous studies have shown[3] that the preferred geometry for the pyrene excimer, Er, is the "sandwich"-like configuration which allows maximum overlap of the π orbitals of a pyrene singlet (^{1}P) and P. Both polarity and viscosity of isotropic solvents can influence the stablity of the excimer.[4] Theoretical calculations[5] suggest that altering solvent polarity changes the relative importance of charge-transfer ($[P_1^+P_2^-]$ and $[P_1^-P_2^+]$) and excitation resonance ($[P_1^*P_2]$ and $[P_1P_2^*]$) contributions, thus modifying the electronic nature of the complex. In contrast, high solvent viscosity increases excimer stability by inhibiting molecular motions which distort the complex from its preferred, symmetrical configuration to less symmetrical, nonparallel orientations.[4b,6] Thus,

(1) Part 7: Otruba, J. P., III; Weiss, R. G. *Mol. Cryst. Liq. Cryst.* **1982**, *80*, 165.

(2) Anderson, V. C.; Craig, B. B.; Weiss, R. G. *J. Am. Chem. Soc.* **1981**, *103*, 7169.

(3) (a) Birks, J. B.; Lumb, M. D.; Munro, I. H. *Proc. R. Soc. London, Ser. A* **1964**, *280*, 289. (b) Chandross, E. A.; Dempster, C. J. *J. Am. Chem. Soc.* **1970**, *92*, 3586. (c) Mataga, N.; Torihashi, Y.; Ota, Y. *Chem. Phys. Lett.* **1967**, *1*, 385.

(4) (a) Beens, H.; Weller, A. *Chem. Phys. Lett.* **1969**, *3*, 666. (b) Birks, J.; Alwattar, A.; Lumb, M. *Ibid.* **1971**, *11*, 89. (c) Beens, H.; Weller, A. In "Organic Molecular Photophysics"; Birks, J., Ed.; Wiley: New York, 1973; Vol. 2, Chapter 4.

(5) (a) Murrell, J. N.; Tanaka, J. *Mol. Phys.* **1964**, *4*, 363. (b) Smith, F. J.; Armstrong, A. T.; McGlynn, S. P. *J. Chem. Phys.* **1966**, *44*, 442. (c) Chandra, A. K.; Lim, E. C. *J. Chem. Phys.* **1968**, *49*, 5066.

(6) Birks, J. B. In "The Exciplex"; Gordon, M., Ware, W. R., Eds.; Academic Press: New York, 1975.

0002-7863/82/1504-2972$01.25/0

Table I.[a] Effect of Pyrene Concentration on the Slopes from Figures 1 and 3a as a Function of Phase and on CM Transition Temperatures

		E_a,[b] kcal/mol				$R[\mathrm{d} \ln I^P/\mathrm{d}(1/T)]$,[c] kcal/mol	
[P], M	$T_{c \rightarrow i}$, °C	cholesteric phase		isotropic phase		cholesteric phase	isotropic phase
0.012	57–57.5	1.6 ± 0.1		2.2 ± 0.1			
0.050	55–55.5	4.4 ± 0.2		5.3 ± 0.2		6.2 ± 0.6	4.2 ± 1.6
0.10	53–53.5	5.9 ± 0.1		5.8 ± 0.1			
0.14	52–52.5	6.6 ± 0.1		5.7 ± 0.2			
0.14[d]	49–49.5	(6.4 ± 0.1)	6.5 ± 0.3	(5.5 ± 0.2)	5.6 ± 0.5		
0.16	51.5–52	6.7 ± 0.1		5.5 ± 0.1		5.0 ± 0.2	9.6 ± 0.4
0.17	49–49.5	6.8 ± 0.1		5.1 ± 0.3			
0.19	48–48.5	6.3 ± 0.1		5.0 ± 0.3		10.6 ± 0.8	13.6 ± 2.6
0.22	46–46.5	6.6 ± 0.2		6.4 ± 0.1		9.8 ± 0.2	11.0 ± 0.6

[a] Errors are expressed as standard deviations. [b] See eq 16 and 17. [c] See eq 12 and 13. [d] 0.03 M *n*-butyl stearate added.

deactivation pathways (intersystem crossing and radiationless decay to the ground state) are restricted by the viscosity of the solvent.[7]

The efficiency of ^{1}P quenching by P in the cholesteric and isotropic phases will be a sensitive function of two parameters: diffusion of the pyrene moiety and solvent order. While the relative orientations for collisions between ^{1}P and P are unrestricted in an isotropic solvent, a cholesteric phase is expected to mediate solute motions, making some ^{1}P–P collisions (e.g., those in which the two pyrene molecules are plane parallel, as in Er, or coparallel) more probable than others. Furthermore, the extent of solvent reorganization in an Er-like quenching transition state would be small in the cholesteric phase, and each ^{1}P–P encounter would lead to quenching with near unit efficiency (vide infra). On the basis of space-filling (CPK) molecular models and crystal-packing considerations, the plate-like P should reside preferentially in or between the parallel solvent layers of a cholesteric phase. If quenching of ^{1}P by a diffusion-dependent process[8] were to result from rather specific, out-of-plane collisions between ^{1}P and P, its efficiency would be decreased by a cholesteric phase.[2] It would be small even if the geometry required for quenching were relatively nonspecific since CM is very viscous. As mentioned, this has been shown not to be the case; in isotropic media the preferred quenching geometry is believed to be similar to Er.[3,9]

In this paper, dynamic and steady-state quenching of ^{1}P in the cholesteric and isotropic phases of CM is examined. The effect of solvent order on the excimer-like quenching geometry is shown to be minimal and a diffusional model satisfactorily accounts for the data. The results are compared to ^{1}P quenching by CA and the photodimerization of acenaphthylene in which cholesteric order decreases and increases, respectively, the efficiency of reaction.

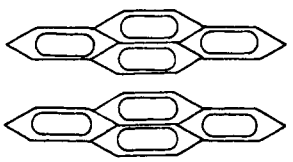

Er

Experimental Section

Melting points and transition temperatures are corrected and were obtained on a Kofler micro hot-stage microscope with polarizing lenses. Pyrene (Aldrich, 99+%), recrystallized twice from ethanol, mp 150–151 °C (lit.[9a] mp 152–153 °C), displayed strictly single exponential fluorescence decays and emission spectra which were indistinguishable from those in the literature.[10] Cholesteryl chloride, cholesteryl nonanoate, and cholesteryl oleate were purified as described previously.[2]

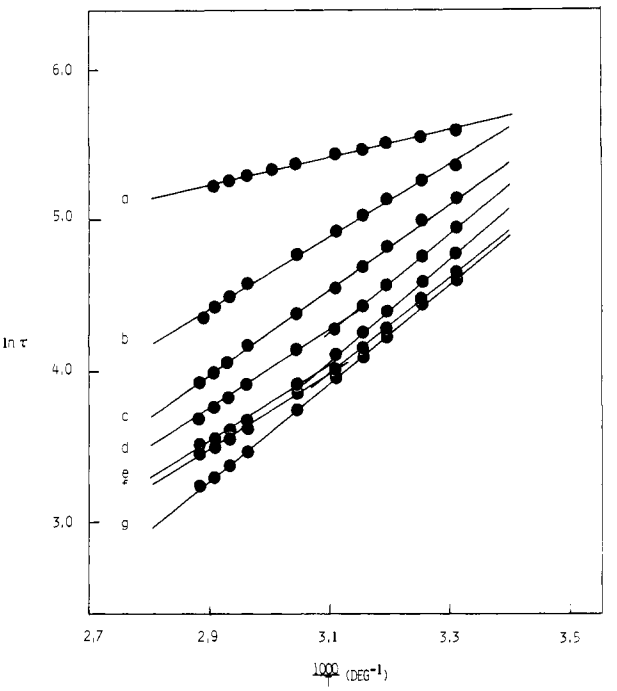

Figure 1. Logarithm of decay constants for pyrene monomer emission vs. the inverse of temperature in CM for [P] = 0.012 M (a), 0.05 M (b), 0.10 M (c), 0.14 M (d), 0.17 M (e), 0.19 M (f), and 0.22 M (g). Data points for 0.16 M P omitted for clarity.

Dynamic Measurements. Samples were mixed and stirred in the isotropic phase of CM until homogeneous. Approximately 30 mg were placed in 0.4-mm flat Pyrex capillary tubes which were flame sealed after several heat (to isotropic temperatures)–pump–cool cycles at ca. 0.05 torr. Decay constants (λ_{excit} 340 nm, λ_{emis}(^{1}P) 400 ± 5 nm, and λ_{emis}(Er) 500 ± 5 nm) were measured by using a single-photon counter described previously.[2] An emission counting efficiency of <5% was maintained to avoid two photon events.[11] The sample temperature was constant (±0.5 °C) as determined by a calibrated thermistor. A 10^{-5} M solution of quinine bisulfate in 0.1 N H_2SO_4 gave τ 19.3 ns (lit.[11] τ 19.4 ns).

Steady-State Fluorescence Measurements. Steady-state fluorescence spectra (uncorrected) were recorded on a Perkin-Elmer MPF-2A spectrophotofluorimeter using the samples from the dynamic studies. The tubes were attached to a thermostated (±0.5 °C) sample holder held at 45° to the 310-nm excitation beam and were not moved while the temperature was varied.

Helical Pitch Measurements.[12] Samples were placed between quartz plates (coated with (*N*-methyl-3-aminopropyl)methoxysilane[13]) separated by a 0.025-mm Teflon spacer. Pitch band measurements were taken at several cholesteric temperatures on a Cary 14 spectrophotometer and are

(7) Electron transfer, another mode of excimer deactivation, is unimportant in nonpolar solvents like CM (Gary, L. M.; deGroot, K.; Jarnagin, R. C. *J. Chem. Phys.* **1968**, *49*, 1577).

(8) (a) Birks, J. B. "Photophysics of Aromatic Molecules"; Wiley-Interscience: New York, 1970, Chapter 7. (b) Birks, J. B. *Rep. Prog. Phys.* **1975**, *38*, 903. (c) Birks, J. B.; Dyson, D. J.; Munro, I. H. *Proc. R. Soc. London, Ser. A* **1963**, *275*, 575.

(9) (a) Birks, J. B.; Kazzaz, A. A.; King, T. A. *Proc. R. Soc. London, Ser. A* **1965**, *291*, 556. (b) Förster, Th.; Seidel, H.-P. *Z. Phys. Chem. (Wiesbaden)* **1965**, *45*, 58. (c) Goldschmidt, C. R.; Ottolenghi, M. *J. Phys. Chem.* **1970**, *74*, 2041.

(10) (a) Nakajima, A. *Bull. Chem. Soc. Jpn.* **1971**, *44*, 3272. (b) Nakajima, A. *Spectrochim. Acta, Part A* **1974**, *30A*, 860. (c) Nakajima, A. *J. Mol. Spectrosc.* **1976**, *61*, 467.

(11) Yguerabide, J. *Methods Enzymol.* **1972**, *26*, Chapter 24.

(12) (a) Baessler, H.; Labes, M. M. *Mol. Cryst. Liq. Cryst.* **1970**, *6*, 419. (b) Adams, J. E.; Haas, W. E. *Ibid.* **1971**, *15*, 27.

(13) Kahn, F. J. *Appl. Phys. Lett.* **1973**, *22*, 386.

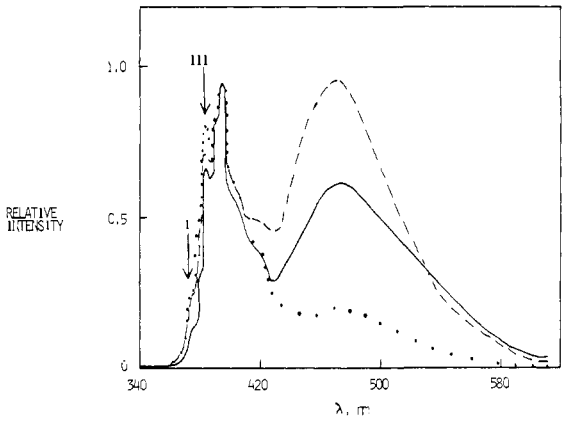

Figure 2. Emission spectra (uncorrected) for [P] = 0.05 M (···), 0.17 M (—), and 0.22 M (---) in CM at 34.5 °C normalized at 393 nm.

estimated to be accurate to ±5 nm.

Results and Discussion

Dynamic Measurements. Lifetimes of ^1P in CM were determined by single-photon counting techniques.[14] Strictly single exponential decays were obtained over at least 3 half-lives for 0.012–0.22 M P in the cholesteric and isotropic phases of CM and were analyzed as described previously.[2] Lifetimes were typically measured from low to high temperatures and then reproduced from high to low. No sample decomposition was evident since lifetimes (τ) were usually reproducible within ±1 ns.

Plots of ln τ vs. $1/T$ are shown in Figure 1. As observed earlier with ^1P quenching by CA, some of the plots exhibit a change in slope at or near the transition temperature (Table I). The slopes could be fit reasonably to no more than two straight lines at any P concentration. Duplicate analyses on the same sample and, in a few cases, on different samples of identical concentration, produced indistinguishable results.

Kinetic Model. A standard mechanism for ^1P quenching is given in Scheme I. Due to excimer irreversibility[8a,b,15] ($k_4 << k_5 +$ k_6), the lifetime of ^1P is given by eq 7. Figure 1, then, represents

Scheme I

$$P \xrightarrow{h\nu} {}^1P \quad (1)$$

$$^1P \xrightarrow{k_1} P + h\nu' \quad (2)$$

$$^1P \xrightarrow{k_2} P \text{ (or } {}^3P) + \Delta \quad (3)$$

$$^1P + P \underset{k_4}{\overset{k_3}{\rightleftharpoons}} Er \quad (4)$$

$$Er \xrightarrow{k_5} 2P + h\nu'' \quad (5)$$

$$Er \xrightarrow{k_6} 2P \text{ (or } {}^3P) + \Delta \quad (6)$$

$$1/\tau = k_1 + k_2 + k_3[P] \quad (7)$$

$$I^P = c\frac{k_1}{k_1 + k_2 + k_3[P]} = ck_1\tau \quad (8)$$

$$I^E = c'\frac{k_3[P]}{k_1 + k_2 + k_3[P]}\frac{k_5}{k_5 + k_6} \quad (9)$$

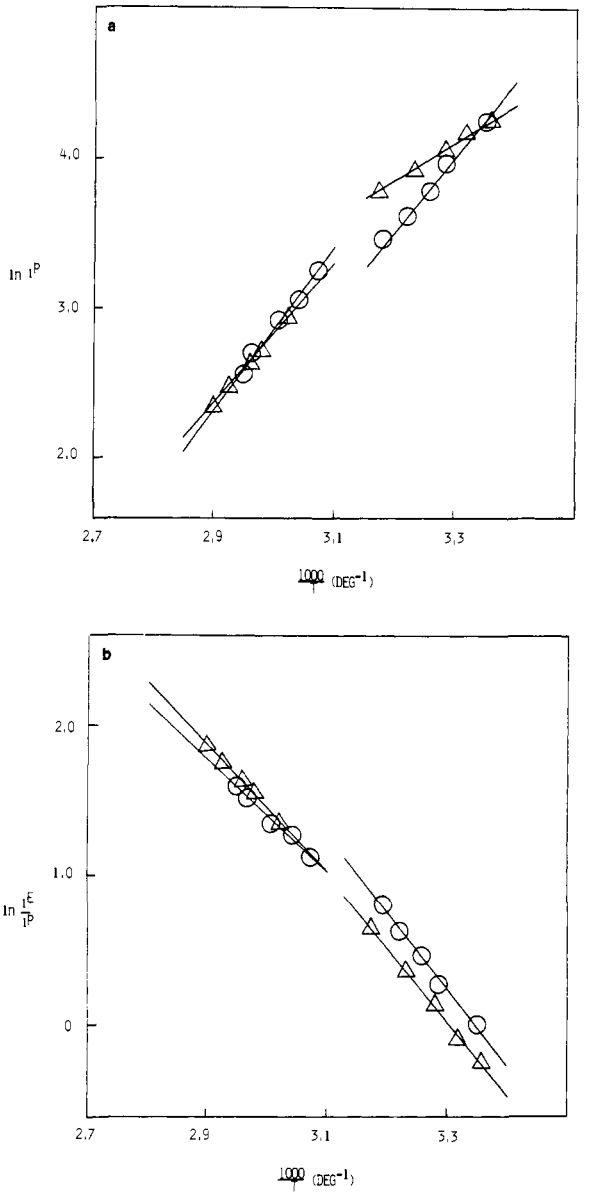

Figure 3. (a) Logarithm of P fluorescence intensity vs. the inverse of temperature for [P] = 0.17 M (Δ) and 0.22 M (○). (b) Logarithm of the ratio of excimer to pyrene singlet emission vs. the inverse of temperature for [P] = 0.17 M (Δ) and 0.22 (○).

Arrhenius plots in which the slopes are equal to E_a/R, the *apparent* activation energy for ^1P quenching divided by the gas constant (eq 16 and 17; vide infra). The linearity of the data is not demanded by the kinetic analysis and suggests that some of the rate constants are small, temperature independent, or vary with temperature in a parallel manner. The E_a in each phase are given in Table I.

Steady-State Measurements. Normalized fluorescence spectra of deaerated solutions of P in CM at 34.5 °C are shown in Figure 2. The III/I intensity ratio of ^1P vibronic bands indicates that ^1P fluoresces in a relatively nonpolar environment[16] and resides preferentially in a region removed from the ester linkages of CM. The broad, structureless emission centered at ca. 470 nm is characteristic of the pyrene excimer.[17] This assignment is substantiated by the dependence of the intensity of the red-shifted emission on P concentration.

Static Quenching Considerations. The steady-state emission intensity of the pyrene monomer (I^P) is expressed in eq 8. Plots of ln I^P vs. $1/T$ at several concentrations of P are displayed in

(14) (a) Ware, W. R. in "Creation and Detection of the Excited State", Part A: Lamola, A. A., Ed.; Marcel Dekker: New York, 1971; Vol. 1, Chapter 5. (b) Knight, A. E. Q.; Selinger, B. K. *Aust. J. Chem.* **1973**, *26*, 1. (c) Lewis, C.; Ware, W. R.; Doemeny, L. J.; Nemzek, T. L. *Rev. Sci. Instrum.* **1973**, *44*, 107.

(15) (a) Birks, J. B.; Srinivasan, B. N.; McGlynn, S. P. *J. Mol. Spectrosc.* **1968**, *27*, 266. (b) Georgescauld, D.; Desmasez, J. P.; Lapouyade, R.; Babeau, A.; Richard, H.; Winnik, M. *Photochem. Photobiol.* **1980**, *31*, 539. (c) Birks, J. In "Organic Molecular Photophysics", Birks, J., Ed.; Wiley: New York, 1973; Vol. 2, Chapter 9.

(16) Kalyanasundaraman, K.; Thomas, J. K. *J. Am. Chem. Soc.* **1977**, *99*, 2039.

Table II. Activation Parameters

	cholesteric			isotropic		
method	E_3, kcal/mol	A_3, M^{-1} s^{-1}	$\Delta S^{\ddagger}$, eu	E_3, kcal/mol	A_3, M^{-1} s^{-1}	$\Delta S^{\ddagger}$, eu
a	9.6 ± 0.6	$(3.6 \pm 2.6) \times 10^{14}$	+7 ± 2	7.5 ± 0.9	$(1.7 \pm 1.7) \times 10^{13}$	+0.5 ± 3
b	8.9 ± 0.4	$(9.2 \pm 3.9) \times 10^{13}$	+3 ± 0.5	6.6 ± 0.6	$(2.1 \pm 0.6) \times 10^{12}$	−4 ± 0.5
c	9.4 ± 2			6.9 ± 2		

[a] From eq 17 and using $(k_1 + k_2) \simeq 3.2 \times 10^6$ s^{-1} in the cholesteric phase and $(k_1 + k_2) \simeq 3.8 \times 10^6$ s^{-1} in the isotropic phase of CM. Errors are expressed as standard deviations from the mean. [b] E_3 calculated from the slopes of Arrhenius plots with the error expressed as standard deviations. A_3 calculated from the corresponding intercept in which the error represents the deviation from the mean, using maximum and minimum Stern–Volmer k_3 values. $\Delta S^{\ddagger}$ determined from the corresponding Eyring plots with the error calculated in a manner analogous to that of A_3. [c] Values obtained from steady-state plots of $\ln I^E/I^P$ vs. $1/T$. Error given is standard deviation from the mean.

Figure 3a, and the slopes are collected in Table I. Differentiation of $\ln I^P$ (eq 8) with respect to $1/T$ yields eq 10. In this expression, c is actually a sum of terms and represents the contributions due to scattering of the excitation light by the cholesteric phase and any solute concentration contributions.

$$\frac{d \ln I^P}{d(1/T)} = \frac{d \ln c}{d(1/T)} + \frac{d \ln k_1}{d(1/T)} + \frac{d \ln \tau}{d(1/T)} \quad (10)$$

$$\frac{d \ln I^P}{d(1/T)} \simeq \frac{d \ln c}{d(1/T)} + \frac{d \ln \tau}{d(1/T)} \quad (11)$$

The temperature-independent nature of k_1 reduces eq 10 to eq 11. Thus, slopes of steady-state and dynamic temperature-dependent data should be equal if (1) the change in solvent birefringence and surface ordering effects are negligible over this temperature range (i.e., $d \ln c/d(1/T) \simeq 0$) and (2) static quenching is unimportant.

Ground-state complexes of pyrene have not been observed in solution.[8,17] However, at concentrations greater than 0.10 M P, a simple statistical model predicts that at the moment of excitation, a nonnegligible group of pyrene molecules may be nearest neighbors, resulting in nondiffusional (static) quenching.[18] Dynamic decay constants will, of course, be unaffected by static quenching contributions. Therefore, at least some of the differences in dynamic and steady-state slopes can be attributed to a static quenching component.

Determination of Activation Parameters. a. From Steady-State Data. Fluorescence intensity measurements at several temperatures and a single P concentration[19] allow E_3, the activation energy for ^1P quenching (and, presumably, excimer formation), to be determined. From Scheme I, the intensities of ^1P and excimer emission are expressed by eq 8 and 9, respectively, where c and c' are constants. The ratio of excimer to ^1P emission is then given by eq 12. Since $k_5 + k_6$ and k_1 are known to be virtually temperature independent,[4b] substitution of an Arrhenius expression for k_3 in eq 12 gives eq 13. Therefore, the slopes of plots of $\ln (I^E/I^P)$ vs. $1/T$ (Figure 3b) yield $-E_3/R$. Average values of E_3 in the cholesteric and isotropic phases obtained from samples of four different P concentrations are collected in Table II.

$$\frac{I^E}{I^P} = \frac{c'k_5}{ck_1}\left(\frac{k_3[P]}{k_5 + k_6}\right) \quad (12)$$

$$\frac{I^E}{I^P} = \frac{c'k_5[P]}{ck_1(k_5 + k_6)} A_3 e^{-E_3/RT} \quad (13)$$

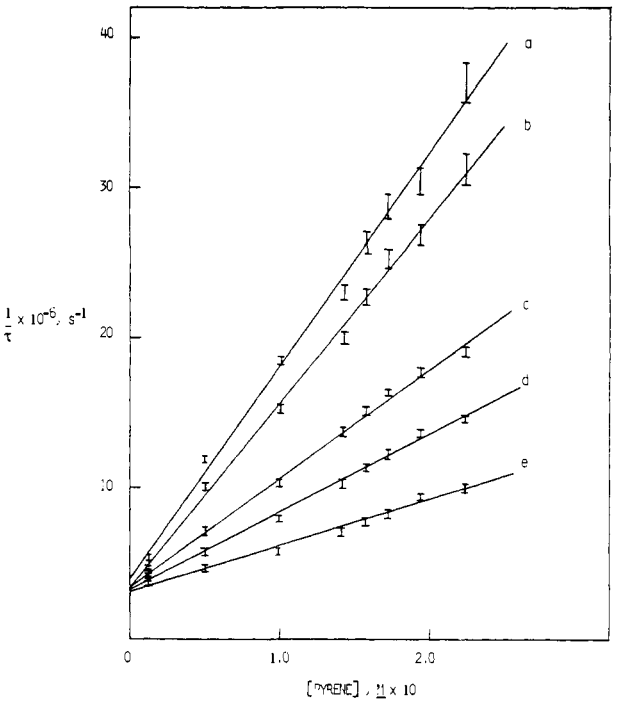

Figure 4. Representative dynamic Stern–Volmer plots for quenching pyrene singlets by P in the isotropic (71 °C (a); 64.5 °C (b)) and cholesteric (48.5 °C (c); 40 °C (d); 29 °C (e)) phases of CM. Error bars represent ±1 ns precision.

b. From Dynamic Data. The expressions which relate E_1, E_2, and E_3 (the activation energies associated with eq 2–4) and the corresponding preexponential A factors to experimental parameters were derived previously[2] and are given in eq 14–17. When the lifetimes of ^1P and Er can be measured, several methods are available for the determination of the individual rate constants and the associated activation parameters.

$$\ln \tau = -\ln (k_1 + k_2 + k_3[P]) \quad (14)$$

$$\ln \tau = -\ln (A_1 e^{-E_1/RT} + A_2 e^{-E_2/RT} + A_3[P] e^{-E_3/RT}) \quad (15)$$

$$\frac{d \ln \tau}{d(1/T)} = \frac{A_1E_1e^{-E_1/RT} + A_2E_2e^{-E_2/RT} + A_3E_3[P]e^{-E_3/RT}}{R(A_1e^{-E_1/RT} + A_2e^{-E_2/RT} + A_3[P]e^{-E_3/RT})} \quad (16)$$

$$E_a = \frac{A_1E_1e^{-E_1/RT} + A_2E_2e^{-E_2/RT} + A_3[P]E_3e^{-E_3/RT}}{A_1e^{-E_1/RT} + A_2e^{-E_2/RT} + A_3[P]e^{-E_3/RT}} \quad (17)$$

From eq 7, it is clear that extrapolation of plots of $1/\tau$ vs. [P] (Figure 4) to zero concentration yields $k_1 + k_2$ in either the cholesteric or isotropic phases of CM. The values determined from these plots are $(3.2 \pm 0.2) \times 10^6$ and $(3.8 \pm 0.3) \times 10^6$ s^{-1} in the cholesteric and isotropic phases, respectively (cf. $k_1 + k_2 \simeq 5.6 \times 10^5$ s^{-1} in liquid paraffin[20]). Substituting $k_1 + k_2$ and the actual values of τ at a given temperature from the dynamic plots (Figure

(17) (a) Förster, Th.; Kasper, K. *Z. Phys. Chem. (Wiesbaden)* **1954**, *1*, 275. (b) Birks, J. B.; Christophourou, L. G. *Spectrochim. Acta* **1963**, *19*, 401.

(18) (a) Wagner, P. J. In "Creation and Detection of the Excited State", Part A: Lamola, A. A., Ed.; Marcel-Dekker: New York, 1971; Vol. 1, Chapter 4. (b) Ware, W.; Lewis, C. *J. Chem. Phys.* **1972**, *57*, 3546. (c) Weller, A. In "Progress in Reaction Kinetics"; Porter, G., Ed.; Pergamon: New York, 1961; Vol. 1, Chapter 7.

(19) Previous studies of fluorescence intensities in liquid crystals have produced erratic results. [Novak, T. J.; MacKay, R. A.; Poziomek, E. J. *Mol. Cryst. Liq. Cryst.* **1973**, *20*, 213.] This is most likely due to surface ordering effects and solvent birefringence which changes as a function of temperature, sample, and even sample placement in the spectrophotofluorimeter.[2] Therefore, static Stern–Volmer plots were not constructed.

(20) Stevens, B.; Thomaz, M. F.; Jones, J. *J. Chem. Phys.* **1967**, *46*, 405.

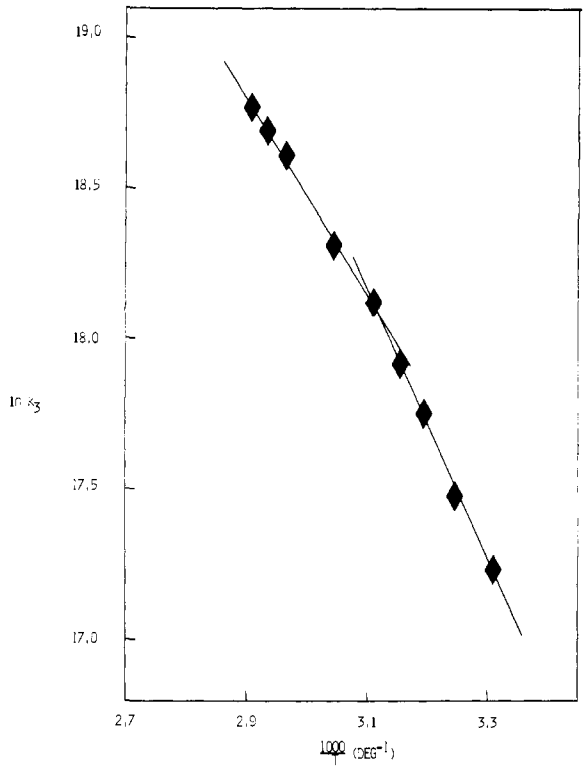

Figure 5. Arrhenius activation plot of ln k_3 vs. the inverse of temperature.

1) into eq 16 allows the best-fit values of E_3 and A_3 in both phases to be calculated at each concentration.[21] E_3 and A_3 obtained in this manner are approximately constant and are given in Table II. The slopes of dynamic Stern–Volmer plots (Figure 4) allow an independent calculation of k_3. An Arrhenius plot of the k_3 values so obtained (Figure 5) yields $-E_3/R$ and ln A_3 from the slope and intercept, respectively (Table II). Both of these determinations make E_3(cholesteric) ca. 2 kcal/mol greater than E_3(isotropic) and A_3(cholesteric) ca. tenfold greater than A_3(isotropic) ($\Delta\Delta S^{\ddagger} \simeq 7$ eu). The magnitude of the E_3 values from dynamic and steady-state methods are within experimental error.

General Medium Considerations. A cholesteric liquid-crystalline phase consists of nematic-like layers arranged in a macroscopic helix, each layer being twisted with respect to the one above and below. Pitch band measurements[22] of CM doped with various concentrations of P indicate that no large changes in macroscopic order occur over the concentration and temperature range of our measurements: pitch band maxima vary from ca. 5000 to 7000 Å.

Above the cholesteric to isotropic transition temperature, the long-range anisotropy of the cholesteric phase is destroyed. Although some short-range order is known to persist,[23] it is unlikely to have a large effect on the rates and specificities of bimolecular processes, like ^{1}P–P quenching, which depend upon diffusion.[8]

Effect of CM on Pyrene Excimer Formation. Previous studies have shown that the probability for excimer formation per ^{1}P–P collision (quenching event) is $\simeq 1$ in low molecular weight isotropic solvents.[3a,8c,24] It is likely, therefore, that diffusional quenching of ^{1}P fluorescence in CM can be ascribed to an excimer-like orientation of ^{1}P and P, similar to Er. The most stable interplanar distance for Er is calculated to be ca. 3 Å.[9a]

It should be noted that ^{1}P–P quenching complexes cannot be distinguished from the excimer by our techniques since in a nonpolar, viscous solvent like CM, each encounter leads irreversibly to excited state complex formation. Therefore, *if* collision complexes are discrete intermediates, they must be converted with unit efficiency to excimer. This fact has been incorporated into the kinetic scheme by deletion of a step in which a collision complex (formally the product of the k_3 step) is converted completely to an excimer. It is possible that the quenching complex and excimer are distinguishable species in more polar solvents capable of supporting radical ions.

On the basis of crystal-packing considerations,[25] pyrene is predicted to be incorporated into the cholesteric phase with its long molecular axis parallel to those of the cholesteryl derivatives which comprise CM. CPK space-filling models indicate that P will lie preferentially parallel to or within the cholesteric solvent layers. Three different types of diffusion, each having a different diffusion coefficient,[26] are expected in this solvent phase. The preferred one for P is most likely perpendicular to the helical screw axis of the phase.[27]

Formation of an excimer-like quenching complex, then, may result from collisions of ^{1}P and P in which both molecules are located in adjacent solvent layers or in which one molecule is in a solvent layer and the other is no more than one layer away. In either case, the relative orientations of ^{1}P and P in an excimer-like quenching complex would not result in a large solvent disruption and, as a result, the solvent layers are not expected to impose a large free energy barrier to quenching.

The approximately constant value of E_3 (see Table II) observed in the cholesteric phase of CM, as solvent order is disrupted by increasing [P], indicates that solvent layering does not appreciably hinder formation of the ^{1}P–P quenching geometry. The small difference in the average values of E_3 between the two phases may be attributed (1) to viscosity differences, the cholesteric being the more viscous medium, and (2) to a much smaller extent, to solvent order disruption upon formation of the transition state. When ^{1}P is quenched by CA, both effects are nonnegligible. In the case of ^{1}P–P quenching, the contribution of solvent order disruption to the relative magnitude of E_3(cholesteric) is small and is confirmed in Table II by the similarity of A_3(cholesteric) and A_3(isotropic) (and, ergo, the small differences between $\Delta S^{\ddagger}$(cholesteric) and $\Delta S^{\ddagger}$(isotropic)). If the transition state for ^{1}P quenching were sufficiently bulky so as to cause a large solvent order disruption, A_3 in the cholesteric phase would be *much* larger than in the isotropic.[2]

These results also predict that addition of a solute which disrupts cholesteric order will not affect the quenching efficiency of ^{1}P by P. Accordingly, we have followed the quenching of ^{1}P in CM containing 0.14 M P and 0.03 M *n*-butyl stearate, a solute which disrupts the cholesteric order (and, to a lesser extent, the viscosity), but does not affect k_1 and k_2.[28] Comparison of this data with that of an identical sample without *n*-butyl stearate (Table I) reveals no discernible difference in E_3(cholesteric) or A_3(cholesteric). Therefore, P quenching of ^{1}P in CM appears to be a diffusion-limited process in which cholesteric order plays little (if any) role: the collisional orientations easily available to ^{1}P and P must be those required for quenching.

(21) Although the E_a in Table I for [P] < 0.10 M are lower than the limiting average value, the calculated E_3 and A_3 are within experimental error of those determined from E_a at higher concentrations. The observed deviation of E_a is due to the nonnegligible contribution of the concentration independent terms of eq 17 (i.e., at low [P], $E_a \neq E_3$).

(22) (a) Fergason, J. L. *Mol. Cryst.* **1966**, *1*, 293. (b) Adams, J.; Haas, W. *Mol. Cryst. Liq. Cryst.* **1972**, *16*, 33.

(23) (a) Yang, C. C. *Phys. Rev. Lett.* **1972**, *28*, 955. (b) Crooker, P. P.; Laidlaw, W. G. *Phys. Rev. A* **1980**, *21*, 2174. (c) Mahler, D. S.; Keyes, P. H.; Daniels, W. B. *Phys. Rev. Lett.* **1976**, *36*, 491.

(24) (a) Speed, R.; Selinger, B. *Aust. J. Chem.* **1969**, *22*, 9. (b) Alwattar, A. H.; Lumb, M. D.; Birks, J. B. In "Organic Molecular Photophysics"; Birks, J., Ed.; Wiley: New York, 1973; Vol. 1, Chapter 8.

(25) (a) Gibson, H. W. In "Liquid Crystals: The Fourth State of Matter"; Saeva, F. D., Ed.; Marcel Dekker: New York, 1979; Chapter 3. (b) Gray, G. W. "Molecular Structure and Properties of Liquid Crystals"; Academic Press: New York, 1962.

(26) (a) Yun, C. K.; Fredrickson, A. G. *Mol. Cryst. Liq. Cryst.* **1970**, *12*, 73. (b) Pochan, J. M. In "Liquid Crystals: The Fourth State of Matter"; Saeva, F. D., Ed.; Marcel Dekker: New York, 1979; Chapter 7. (c) Jost, W. "Diffusion in Solids, Liquids, Gases"; Academic Press: New York, 1960.

(27) Rate constants for diffusion have, unfortunately, not been measured in this direction.

(28) Evidence that *n*-butyl stearate does disrupt CM cholesteric order is found in the transition temperatures. Addition of 0.03 M *n*-butyl stearate lowers the cholesteric–isotropic transition by 3 °C, the same decrease observed upon addition of a 0.03 M P increment.

Comparison of ^{1}P–P Quenching with ^{1}P–CA Quenching and Acenaphthylene Photodimerization. Previously, with CA as quencher, we explained why A(cholesteric) >> A(isotropic) precludes mechanistic models which disregard cholesteric order. Crystal-packing considerations and CPK space-filling models indicate that in order for a P–CA exciplex-like quenching geometry to be attained in the cholesteric phase of CM, adjacent solvent layers must be disturbed. Furthermore, only if one of the components tilts out of the phase is effective overlap between the nitrogen lone-pair orbital and the π system of ^{1}P (the exciplex geometry[29]) achieved. Therefore, the solvent order decreases quenching efficiency by making the orientations appropriate for P–CA quenching less accessible. The overall effect is to increase the entropy of activation and energy of activation in the cholesteric phase.

In contrast, the quantum efficiency for the photodimerization of acenaphthylene is dramatically increased by the order of a cholesteric liquid-crystalline solvent.[30] Incorporation of the planar acenaphthylene in or between layers of the cholesteric phase and preferential plane-parallel diffusion of the solute results in an increased fraction of collisions which lead to products. Thus, cholesteric order facilitates the formation of the photodimer products.

The same diffusional motions and preferred collisional orientations apply to ^{1}P–P quenching and acenaphthylene dimerization when the reactions are conducted in cholesteric liquid-crystalline solvents. Diffusion parallel to the planes of the cholesteric layers results in collisional complexes from which quenching or product formation can proceed.

Dimerization of acenaphthylene is a relatively inefficient process in nonpolar, isotropic solvents, while the efficiency of ^{1}P–P quenching (i.e., quenching events per ^{1}P–P encounter) is near unity. Therefore, an increase in quenching efficiency in the cholesteric phase is not possible, and only if diffusion in the cholesteric phase of CM is less difficult than in its isotropic phase will E_3 be lowered. The increased viscosity of cholesteric CM relative to its isotropic phase makes this impossible.

A comparison of these three studies gives a general indication of the effects which can be expected when bimolecular reactions are conducted in cholesteric liquid-crystalline media. If the isotropic reaction probability per encounter is less than unity, the ordering of solutes imposed by the cholesteric phase may result in an increase or decrease in reaction efficiency. If the phase orients the reactants such that collisions leading to product are more probable (as in the acenaphthylene case), reaction probability will be increased. If, on the other hand, the cholesteric phase makes the preferred collisions less probable (as in the ^{1}P–CA case), the efficiency of the reaction is decreased. Finally, if the reaction probability per encounter in the isotropic phase is near unity, the presence of solvent order can result in a decreased or unchanged (as in the ^{1}P–P case) reaction efficiency.

Conclusions

Employing methods developed recently, analyses of dynamic and steady-state fluorescence data indicate that the relative orientations for ^{1}P quenching by P and excimer formation are similar in the cholesteric and isotropic phases of CM. That E_3(cholesteric) is only slightly greater than E_3(isotropic) and A_3(cholesteric) is slightly larger than A_3(isotropic) suggest that decreased ^{1}P quenching efficiency in the cholesteric phase is a result of increased viscosity. Space-filling models (CPK) and crystal-packing considerations indicate that formation of an excimer-like transition state for quenching, in which the molecules are oriented parallel to one another and to the planes of the cholesteric phase, does *not* significantly disrupt solvent order. Comparison of these data and those for ^{1}P quenching by CA and photodimerization of acenaphthylene demonstrate that a cholesteric liquid-crystalline medium can be used to differentiate various quenching transition-state geometries on the basis of their shapes. Investigations in which exciplex formation is expected to be much more dependent upon the viscosity of a cholesteric phase than its order (as in the ^{1}P–P excimer studied here) are in progress.

Acknowledgment. The National Science Foundation (Grant CHE-7906572) and the Naval Research Laboratory are acknowledged for financial support of this research.

Registry No. Pyrene, 129-00-0.

(29) (a) Meeus, F.; Van der Auweraer, M.; Dederen, J. C.; DeSchryver, F. C. *Recl. Trav. Chim. Pays-Bas* **1979**, *98*, 220. (b) Taylor, G. N.; Chandross, E. A.; Schiebel, A. H. *J. Am. Chem. Soc.* **1974**, *96*, 2693.

(30) Nerbonne, J. M.; Weiss, R. G. *J. Am. Chem. Soc.* **1979**, *101*, 409.

Dynamics of Interfacial Electron-Transfer Processes in Colloidal Semiconductor Systems

Dung Duonghong, Jeremy Ramsden, and Michael Grätzel*

Contribution from the Institut de Chimie Physique, Ecole Polytechnique Fēdērale, CH-1015 Lausanne, Switzerland. *Received July 29, 1981*

Abstract: The dynamics of interfacial electron-transfer reactions were studied with colloidal TiO_2 and CdS particles, which form transparent aqueous dispersions. Excitation of the semiconductor was carried out by a nanosecond laser flash and subsequent conduction-band electron (e^-_{CB}) and hole (h^+) transfer reactions to solution species examined by kinetic spectroscopy. Methylviologen (MV^{2+}) was employed as an electron acceptor and thiocyanate or a phenothiazine derivative as a hole scavenger. Excitation of colloidal TiO_2 leads to long-lived e^-_{CB} whose rate of reaction with MV^{2+} is strongly influenced by the MV^{2+} concentration and pH. The pH effect on the yield of MV^+ can be exploited to derive the flat-band potential of the particle for which a value of $E_{fb} = 0.130 - 0.059$(pH) V (vs. NHE) was obtained. In the case of colloidal CdS the lifetime of the electron-hole pair was determined as 0.3 ns from time-resolved fluorescence spectroscopy. Only donors or acceptors adsorbed onto the particle surface can intervene as h^+ or e^-_{CB} scavengers, respectively. Experiments with Pt-loaded CdS established the competition of catalytic H_2 production by e^-_{CB} with electron transfer to adsorbed MV^{2+}. RuO_2 deposits are shown to enhance hole transfer from the valence band to solution species.

Interfacial electron-transfer processes play a crucial role in light-energy conversion devices where semiconductor–electrolyte junctions are employed as light-harvesting units. In view of the importance of these devices for the utilization of solar energy, it is highly desirable to obtain detailed experimental information on the dynamics of photoinduced conduction or valence-band processes involving species in solution. In the case of solid semiconductor electrodes, a direct study of the kinetics of these re-

0002-7863/82/1504-2977$01.25/0